

Progress and Bottlenecks in Simulating Lattice Gauge Theory with Fermions

John B. Kogut¹

We present a progress report in lattice gauge theory computer simulations which includes the effects of light, dynamical fermions. Microcanonical and hybrid microcanonical-Langevin algorithms are presented and discussed. A method for "accelerating" stochastic differential equations and defeating critical slowing down is reviewed. Physics applications such as the thermodynamics of quantum chromodynamics, hierarchical energy scales in unified gauge theories, and the phase diagram of theories with many fermion species are discussed. Prospects for future research are assessed.

KEY WORDS: Lattice gauge theory; computer simulations; critical slowing down, Grassman variables; Langevin equation; microcanonical.

1. LATTICE GAUGE THEORY WITH FERMIONS

The four-dimensional Euclidean action density S for lattice gauge theory with fermions reads generically

$$S = \sum_{ij} \bar{\psi}_i [D(U) + m]_{ij} \psi_j + S_0(U) \quad (1.1)$$

where ψ_i is a Grassman field at site i , $A_{ij} = [D(U) + m]_{ij}$ is the gauge covariant Dirac operator, and $S_0(U)$ is the pure gauge field action on the lattice.⁽¹⁾ The precise form of the gauge covariant discrete difference operator $D(U)$ depends on the lattice fermion method employed. We will be considering staggered fermions⁽²⁾ in this article, so ψ_i will be one component object and the fermion contribution to (1.1) reads

$$\sum_n \bar{\psi}(n) \left\{ \frac{1}{2} \sum_{\mu=1}^4 \eta_{\mu}(n) [U_{\mu}(n) \psi(n + \mu) - U_{\mu}^+(n - \mu) \psi(n - \mu)] + m\psi(n) \right\} \quad (1.2)$$

¹ Department of Physics, University of Illinois at Urbana-Champaign, 1110 West Gren Street, Urbana, Illinois 61801.

where $\eta_\mu(n)$ are phase factors that carry the spin- $\frac{1}{2}$ character of the continuum Dirac field and $U_\mu(n)$ is the $SU(3)$ rotation matrix residing on the link between sites n and $n + \mu$. For the purposes of this discussion all these details are not essential. Suffice it to say that (1.2) has the good feature of describing four species of Dirac fermions which become massless when $m \rightarrow 0$ in a natural fashion. $\langle \bar{\psi}\psi \rangle$ is a good-order parameter for chiral symmetry, one of the two basic quantities (confinement is the other) of interest here.

Since our subject is the status of computer simulations of lattice gauge theory with fermions, our interest focuses on the partition function

$$Z = \int \prod_i d\psi_i \prod_j d\bar{\psi}_j \prod_{n,\mu} dU_\mu(n) \exp(-S) \quad (1.3)$$

Since the ψ_i are anticommuting numbers, a direct simulation of (1.3) is not practical. Instead the fermions can be integrated out of (1.3) since (1.1) is a quadratic form in ψ

$$\begin{aligned} Z &= \int \prod dU_\mu(n) \det[\mathcal{D}(U) + m] \exp[-S_0(U)] \\ &= \int \prod dU_\mu(n) \exp(-S_0(U) + \text{tr} \ln[\mathcal{D}(U) + m]) \end{aligned} \quad (1.4)$$

It is not so clear, however, that this step represents real progress since $\text{tr} \ln[\mathcal{D}(U) + m]$ is an effective, nonlocal interaction among the U variables. Such actions are not well-studied and classified in the context of traditional statistical mechanics approaches to critical phenomena. At least the determinant in (1.4) is positive semidefinite for staggered fermions.

We all recognize the physical origin for the determinant here. It represents closed fermion loops, virtual quark-antiquark pairs, and the plus sign, $+\text{tr} \ln[\mathcal{D}(U) + m]$, in (1.4) is responsible for the perturbation theory rule: -1 for each closed fermion loop.

Various numerical approaches to evaluating (1.4) and physically relevant matrix elements have been proposed. Monte Carlo methods, the so-called pseudo-fermion algorithms,⁽³⁾ are being studied as well as microcanonical^(4,5) and Langevin equations.⁽⁶⁾ I will concentrate on the latter two methods in this review. At this time all such algorithms are controversial—we have not studied enough cases with enough computer power to delineate the clear successes and limitations of each method. However, such studies are being vigorously pursued at this time and solid answers concerning the reliability, scope, and error estimates in each method should be forthcoming.

2. THE MICROCANONICAL ENSEMBLE AND MOLECULAR DYNAMICS

We begin by reviewing the molecular dynamics approach⁽⁴⁾ to problems in equilibrium statistical mechanics. Consider a boson field ϕ which might be defined on a lattice. The theory has an action $S(\phi)$ which determines its path integral and equilibrium statistical mechanics properties. This system has no natural dynamics which would govern its approach to equilibrium. However, it can be given dynamics in several ways—the molecular dynamics and the Langevin equations are two alternatives. In the molecular dynamics approach we associate $S(\phi)$ with a potential $V(\phi) \equiv \beta^{-1}S(\phi)$ and construct a fictitious Hamiltonian

$$H = T + V = \sum_i \frac{1}{2} p_i^2 + V(\phi) \quad (2.1)$$

where i label lattice sites and p_i will soon be interpreted as the momentum conjugate to ϕ_i . Using (2.1) we could consider the classical statistical mechanics based on the invariant phase space $\prod_i dp_i d\phi_i$ and the Boltzmann factor $\exp(-\beta H)$. Since the p_i integrals are trivial, this formulation reduces to the original path integral formulation of the boson field theory.

To give this approach some meat, we identify p_i with the momentum conjugate to ϕ_i by introducing a 5th dimension τ into the problem

$$p_i = d\phi_i/d\tau \quad (2.2)$$

Then the ensemble given by the phase space measure $\prod_i dp_i d\phi_i$ and the Boltzmann factor $\exp(-\beta H)$ defines the usual canonical ensemble of classical statistical mechanics. There is still no advantage in all this until one passes to the microcanonical ensemble. Now the energy is fixed, $H = E$, and the measure in phase space is $\prod_i dp_i d\phi_i \delta(H - E)$. Observables in the system $\theta(p, \phi)$ have expectation values

$$\langle \theta \rangle = \frac{1}{Z} \int \prod_i dp_i d\phi_i \delta(H - E) \theta(p, \phi) \quad (2.3)$$

If θ is just a function of ϕ , then standard arguments apply to show that $\langle \theta \rangle$, calculated in the microcanonical ensemble, is the same as $\langle \theta \rangle$ calculated in the canonical ensemble in the large volume $V \rightarrow \infty$ limit.^(4,5)

But $\langle \theta \rangle$ can also be calculated from the time evolution of the classical system. This is the molecular dynamics approach to the problem. Let

$[\phi(\tau), p(\tau)]$ describe the phase space point of the physical system. Then a time average of θ can be calculated

$$\langle \theta \rangle = \lim_{T \rightarrow \infty} \frac{1}{T} \int_0^T \theta[p(\tau), \phi(\tau)] dt \quad (2.4)$$

This time average reproduces the expectation value (2.3) if the ergodic hypothesis works for this physical system. Roughly speaking, one must assume that the Hamiltonian dynamics of the system carry the phase space point $[\phi(\tau), p(\tau)]$ uniformly over the energy shell $H = E$.

The final ingredient in this molecular dynamics approach is the computation of the coupling β given the system's fixed energy. The necessary correspondence follows from the equipartition theorem for the kinetic energy T

$$\langle T \rangle = \frac{1}{2} \beta^{-1} N \quad (2.5)$$

where N is the number of independent, excited degrees of freedom in the system.

Equation (2.4) and (2.5), coupled with the Hamilton equations of motion following from (2.1) and (2.2), represent a clear alternative to Monte Carlo simulation procedures of pure bose systems. This formulation has several interesting points: (1) It is fully deterministic, (2) it involves ordinary coupled differential equations, and (3) it generalizes to a practical method for fermions. Let's review the fermion method before discussing its strengths and weaknesses further.

Now we wish to invent a classical system in $4 + 1$ dimensions involving only complex numbers whose molecular dynamics generate the path integral equation (1.4) with the infamous fermion determinant. Consider the Lagrangian⁽⁵⁾

$$L = -S_0(U) + \frac{1}{2} \sum_{n,\mu} \dot{U}_\mu^\dagger(n) \hat{P} \dot{U}_\mu(n) + \sum_{ij} \phi_i^\dagger [A^\dagger A]_{ij} \phi_j - \omega^2 \sum_i \phi_i^\dagger \phi_i \quad (2.6)$$

where A is the lattice Dirac operator defined earlier, and \hat{P} is a projection operator $\text{diag}(1, 1, 0)$ which picks out independent variables in the $SU(3)$ matrix \dot{U}_μ . Thus L consists of kinetic energy terms for the gauge fields, the "pseudofermions" ϕ , and potential terms for both. $A^\dagger A$ appears in L rather than A itself to insure positivity. This unusual form for the pseudofermion kinetic energy will generate the fermion determinant with the correct sign. Note that this L is local because A couples only nearest neighbors.

It is straightforward to identify the canonical momentum of this physical system

$$p_{\dot{\mu}}(n) = \dot{U}_\mu(n) \quad P_i = [\phi^\dagger A^\dagger A]_i \quad (2.7)$$

and construct the Hamiltonian

$$H = \frac{1}{2} \sum p^2 + \sum P^\dagger (A^\dagger A)^{-1} P + S_0(U) + \omega^2 \sum \phi^\dagger \phi \quad (2.8)$$

and consider the Hamiltonian equations of motion

$$\begin{aligned} \dot{P}^\dagger &= \frac{d}{d\tau} [A^\dagger(U) A(U) \dot{\phi}] = -\omega^2 \phi \\ \dot{p} = \dot{U} &= -\frac{\partial}{\partial U^\dagger} S_0(U) + \dot{\phi}^\dagger \frac{\partial}{\partial U^\dagger} [A^\dagger(U) A(U)] \dot{\phi} \end{aligned} \quad (2.9)$$

These equations are generic in character. The real equations which are simulated choose a convenient parametrization for the $U_\mu(n)$ matrices and incorporate constraints appropriately.⁽⁷⁾ But the point to be stressed here is simply that (2.9) is a tractable set of coupled ordinary differential equations. The fermions introduce the complication of requiring the solution of a sparse set of linear equations for $\dot{\phi}$ of the form $A^\dagger A \dot{\phi} = \dots$ for each time step. This is done efficiently with good control of errors by standard methods such as the conjugate-gradient algorithm. As the bare quark mass approaches zero, these iterative sparse matrix algorithms require more computer time, but they prove to be quite practical (see the second reference in Ref. 5, for example).

Our last task is to check that L really gives the original path integral. The canonical ensemble based on (2.8) reads

$$Z = \int Du Dp D\phi D\phi^\dagger DP DP^\dagger \exp(-H/T) \quad (2.10a)$$

All the variables except U enter H quadratically, so the integrals can be done

$$Z = \text{const} \int DU \det^2 A(U) \exp[-S_0(U)/T] \quad (2.10b)$$

which is the required answer except for the second power of the determinant. However, since $A^\dagger A$ in the staggered fermion method does not couple nearest-neighbor pseudo-fermion fields, ϕ can be set to zero on every other lattice site (see, e.g., the second reference in Ref. 5).

Now we see clearly the character of the tricks in (2.6) and (2.8). The pseudo-fermion kinetic energy in L is $\frac{1}{2}mv^2$ with $m \sim A^\dagger A$. When the H is constructed we have $p^2/2m$, and the $(A^\dagger A)^{-1}$ here was responsible for the positive power of $\det A^\dagger A$ in (2.10b). The nice feature of this scheme is that

the full nonlocal character of the determinant is avoided by the algorithm. In each time step $A^\dagger A \dot{\phi} = \dots$ is solved for $\dot{\phi}$; this is a local operation since $A^\dagger A$ only couples nearby degrees of freedom.

The last ingredient in the algorithm is the calculation of the coupling constant β . If we identify the number of active, independent degrees of freedom N^* of the system, this can be done using the equipartition theorem

$$\frac{1}{2}\beta^{-1}N^* = \langle T \rangle = \langle \dot{\phi} A^\dagger A \dot{\phi} + \frac{1}{2} \sum \dot{U}^\dagger \hat{P} \dot{U} \rangle \quad (2.11)$$

The calculation of N^* for particular parametrizations of the U matrices is discussed in Ref. 7.

3. MOLECULAR DYNAMICS APPROACH TO THE CANONICAL ENSEMBLE

The “naive” microcanonical fermion and gauge field algorithm of Sec. 2 can be generalized and improved in many ways. Let’s discuss a variation on the original method which has three interesting features:

1. It is completely deterministic.
2. It simulates the canonical ensemble.
3. It treats β as an input, rather than an output, variable.

The idea here is to add 1 df s which will act as a heat bath for the original microcanonical system. If its kinetic and potential energies can be chosen appropriately, properties 1 to 3 follow. Since the new variable changes the system from one at fixed energy to one at fixed temperature, we will call it a “demon” following a similar, but different, idea used for the Ising model.⁽⁸⁾

Let’s illustrate the idea for a set of N point particles⁽¹⁰⁾

$$L = \sum_i \frac{1}{2} m_i \dot{\mathbf{r}}_i^2 - \phi(\{\mathbf{r}\}) \quad (3.1)$$

which could be simulated by the usual molecular dynamics equation. Instead, introduce a demon s and a Lagrangian describing the system of $N+1$ particles

$$L = \sum_i \frac{1}{2} m_i^2 s^2 \dot{\mathbf{r}}_i^2 - \phi(\{\mathbf{r}\}) + \frac{1}{2} Q \dot{s}^2 - (N+1) T \ln s \quad (3.2)$$

and simulate the equations of motion here. To see that the new system described the original N point particles at temperature T , form the Hamiltonian from (3.2)

$$H = \sum_i \mathbf{p}_i^2 / 2m_i s^2 + \phi(\{\mathbf{r}\}) + p_s^2 / 2Q + (N+1) T \ln s \quad (3.3)$$

and consider the microcanonical ensemble

$$Z = \int dp_s ds \prod_i d\mathbf{p}_i d\mathbf{r}_i \delta(H - E) \tag{3.4}$$

Rescale $\mathbf{p} \rightarrow \mathbf{p}/s$, do the s integral using the delta function, and do the p_s Gaussian integral trivially, to find

$$Z = \int \prod_i d\mathbf{p}_i d\mathbf{r}_i \exp \left\{ - \left[\sum_i \mathbf{p}_i^2 / 2m_i + \phi(\{\mathbf{r}\}) \right] / T \right\} \tag{3.5}$$

which is the desired answer.

In retrospect we see that the logarithmic potential for the demon was essential to generate the Boltzmann factor in (3.5).

The nice features of the molecular dynamics simulation of (3.2) are: (1) T can be chosen as an input variable, (2) $1/V$ effects, which distinguish the microcanonical and canonical ensembles, are suppressed, and (3) equipartition can be monitored clearly through $\langle p_s^2 / 2Q \rangle = T/2$.

This approach to field theory simulations has been tested on a number of systems. The two-dimensional planar spin model was simulated by Monte Carlo, naive microcanonical, and the demon algorithms. The average action, topological charge (the theory has a vortex driven phase transition first described by Kosterlitz and Thouless), spin-spin correlation function, and demon kinetic energies were monitored. The Monte Carlo and demon simulations were in excellent agreement on 15^2 and 30^2 lattices and their expectation values differed only at $1/V$ ($V = \text{volume}$) effects from the naive microcanonical results.

The demon trick is easily generalized to gauge theories with fermions. The Lagrangian becomes

$$L = \frac{1}{2} \sum s^2 \text{tr} \dot{U}^\dagger \hat{P} \dot{U} - \beta S_0(U) + \phi^\dagger A^\dagger(U) A(U) \phi - \omega^2 \phi^\dagger \phi / s^2 + \frac{1}{2} Q \dot{s}^2 - (N + 1) T \ln s \tag{3.6}$$

Long runs (15,000 sweeps) have been carried out at $\beta = 6/g^2 = 5.512$ on a 4×8^3 lattice at fermion mass of $m = 0.10$ where there is extensive microcanonical data.⁽⁹⁾ The two algorithms are in very good agreement but the demon results showed less severe long time correlations, as one would hope.

4. FACING ERGODICITY BREAKING SQUARELY

Chemical physicists have considerable experience with molecular dynamic simulations of systems containing 5–50 df. These systems can be

mapped onto a polymer of 5–50 monomers which interact through strong nearest-neighbor harmonic forces perturbed by weaker anharmonic effects. In these cases the simplest molecular dynamic algorithms fail badly because the normal modes do not exchange energy on short enough time scales for practical simulations.⁽¹⁰⁾ In fact, if the anharmonic forces in the system are weak enough the KAM theorem applies, which implies that the system will not sample the energy surface uniformly. In these cases of relatively few degrees of freedom ergodicity breaking is easily monitored in the simulation. The breaking is clear and obvious. In our field theory applications it is harder to monitor potentially disastrous effects such as these. However, in asymptotically free theories where the ultraviolet fixed point lies at vanishing coupling, we must expect trouble with ergodicity as the continuum limit of the lattice theory is made. In addition, at strong coupling where correlation lengths are small ergodicity breaking is also expected. In simulations at intermediate coupling obvious failures of ergodicity have not been found in $SU(2)$ and $SU(3)$ gauge theories on “large” lattices (8^4 , $8^3 \times 16$, 6×12^3 , for example), but some observables have shown dangerous long-time correlations. Certainly the microcanonical algorithm should be improved. In fact, the physical chemists have adopted the molecular dynamics technique to physical systems which are not ergodic. The “quick fix” they use is simply to “refresh” the velocities in the system from time to time, i.e., the velocities $v_i(\tau)$ are put into a Boltzmann distribution at τ_0 and the system is evolved from τ_0 by molecular dynamics to the time $\tau_0 + \tau^*$ where the velocities are “refreshed” again, etc. This method has become the standard for many chemistry problems and has been discussed by Berne, Andersen, and others extensively.^(9,10)

Luckily there is more to such “quick fixes” than just guesswork. They are closely related to Langevin dynamics and can be placed on a solid theoretical footing.⁽¹¹⁾ We will refer to such schemes as “hybrids”—they combine the strong points of the naive microcanonical and the Langevin algorithms into a new, improved method.

Consider a simple example: an action $S(q)$ and a bose variable q .⁽¹¹⁾ We want to calculate an expectation value

$$\langle F(q) \rangle = \frac{1}{Z} \int dq F(q) \exp[-S(q)] \quad (4.1)$$

In the microcanonical approach, the system is given dynamics

$$\ddot{q}(\tau) = -\partial S(q)/\partial q \quad (4.2)$$

and expectation values are replaced by time averages

$$\langle F(q) \rangle = \lim_{T \rightarrow \infty} \frac{1}{T} \int_0^T dt F[q(\tau)] \quad (4.3)$$

In the Langevin approach, the system is given dynamics with explicit white noise

$$\begin{aligned} \dot{q}(\tau) &= -\partial S/\partial q + \eta(\tau) \\ \langle \eta(\tau) \eta(\tau') \rangle &= 2\delta(\tau - \tau') \end{aligned} \tag{4.4}$$

and (4.3) is applied again. The stochastic differential equation (4.4) causes $q(\tau)$ to execute a forced random walk such that it covers phase space with the weight $\exp[-S(q)] dq$.

There is an intimate relation between (4.2) and (4.4), which is best seen by replacing the differential equations by discrete difference equations. The Langevin system becomes, denoting ξ_n as noise

$$\begin{aligned} q_{n+1} &= q_n + \Delta \xi_n - \frac{1}{2} \Delta^2 S'(q_n) \\ \xi_n \xi_{n'} &= \delta_{nn'} \\ \tau_{n+1} - \tau_n &= \frac{1}{2} \Delta^2 \end{aligned} \tag{4.5}$$

while the microcanonical reads

$$\begin{aligned} q_{n+1} &= 2q_n - q_{n-1} - \Delta^2 S'(q_n) \\ \tau_{n+1} - \tau_n &= \Delta \end{aligned} \tag{4.6}$$

which can be written more suggestively as

$$q_{n+1} = q_n + \frac{1}{2}(q_{n+1} - q_{n-1}) - \frac{1}{2} \Delta^2 S'(q_n) \tag{4.7}$$

So, we have the correspondences

Langevin noise	Microcanonical velocity
$\tau_{n+1} - \tau_n = \frac{1}{2} \Delta^2$	$\tau_{n+1} - \tau_n = \Delta$

Each scheme has the following features: (1) Langevin has explicit noise, so it is ergodic by construction. However, it samples the phase space very slowly in many cases because $q(\tau)$ executes a forced random walk which, if the noise term dominates, fills space at a rate $N^{1/2}$, N = number of time steps of (4.5). (2) Microcanonical dynamics follows the classical equations of motion so it is as efficient as possible in probing the important regions of phase space locally. Also, its time step is large, so it moves along its trajectories rapidly. However, it may not be ergodic, i.e., for long times it may get trapped into regions of phase space which are only accessible to the Langevin simulation because of its explicit noise.

All this suggests a hybrid method which combines the best features of both algorithms.⁽¹¹⁾ In the hybrid scheme a time step will be either Langevin (probability $p\Delta$) or microcanonical (probability $1 - p\Delta$)

$$q_{n+1} = q_n + \Delta v_n - \frac{1}{2}\Delta^2 S'(q_n) \quad (4.8a)$$

with

$$v_n = \begin{cases} (q_{n+1} - q_{n-1})/2\Delta & \text{otherwise, probably } p\Delta \\ \xi_n \end{cases} \quad (4.8b)$$

$$\tau_{n+1} = \tau_n + \Delta$$

One can attempt to optimize this algorithm by choosing p appropriately. The generic best choice is to set p to twice the frequency of the "slowest mode" in the system.⁽¹¹⁾ Inspecting the observables of a typical microcanonical run one can find slowly relaxing modes and estimate p . The idea here is the following: The microcanonical algorithm permits the system to sample a finite region of phase space efficiently for a fixed time interval. That time should be as long as the period of the slowest mode in the system. Then it is best to "refresh" the system, so it can move to a completely new region of phase space. This is done with the (relatively unlikely) Langevin step.

These ideas can be implemented for lattice gauge theory with fermions. We begin with the molecular dynamics Lagrangian for lattice gauge theory with fermions

$$L = \frac{1}{2} \sum_{n,\mu} \dot{U}_\mu^\dagger(n) \hat{P} \dot{U}_\mu(n) + \sum_{ij} \phi_i^\dagger [A^\dagger(U) A(U)]_{ij} \phi_j - \omega^2 \sum_i \phi_i^\dagger \phi_i - \beta \sum (\text{tr } UUUU + \text{h.c.}) \quad (4.9)$$

where $A(U)$ is the hopping matrix of staggered fermions, $\hat{P} = \text{diag}(1, 1, 0)$, and ϕ_i is a complex field residing on every other lattice site. To implement the hybrid algorithm on (4.9) we use the fact that \dot{U} , ϕ , and ϕ appear in three quadratic terms. Therefore, at any time step in the evolution of the molecular dynamics equations one can replace the \dot{U} fields, say, by a completely new field configuration in the Boltzmann distribution $\exp(-\frac{1}{2} \sum \dot{U} \hat{P} \dot{U})$ by standard formulas. Similarly ϕ and ϕ can be replaced by new random fields in the appropriate distributions at chosen intervals. Some care must be exercised with ϕ because of the matrix character of the second term in (4.9). Extensive tests and algorithm tuning on small asymmetric lattices which simulate finite temperatures have been made. The expectation value of the pure gauge field action (the plaquette), the Wilson

line (the exponential of minus the excess free energy for a heavy quark in the vacuum), $\langle \bar{\psi}\psi \rangle$ (the chiral symmetry order parameter), and quark and gluon energy densities have been measured. In Fig. 1 we show the time correlation data for the Wilson line. The hybrid algorithm was run with a discrete time step $dt = .02$ for 10,000 sweeps on a 2×4^3 lattice, and noise was applied at regular intervals ranging from every step (Langevin) to every 1000 sweeps. Figure 1 shows that the minimum correlation time occurs when noise is applied every 50 ± 20 sweeps. Since $dt = .02$ this corresponds to a "physical time" of $1 \pm .4$ units. Note that the hybrid algorithm is more than 3.3 times as efficient as the Langevin limit. In fact, the correlation times for all the matrix elements could be reduced to 2 or 3 time units by applying noise to the system at intervals of $.5 - 2$ time units. This favorable result also occurs on larger lattices, 4×8^3 and 6×10^3 .

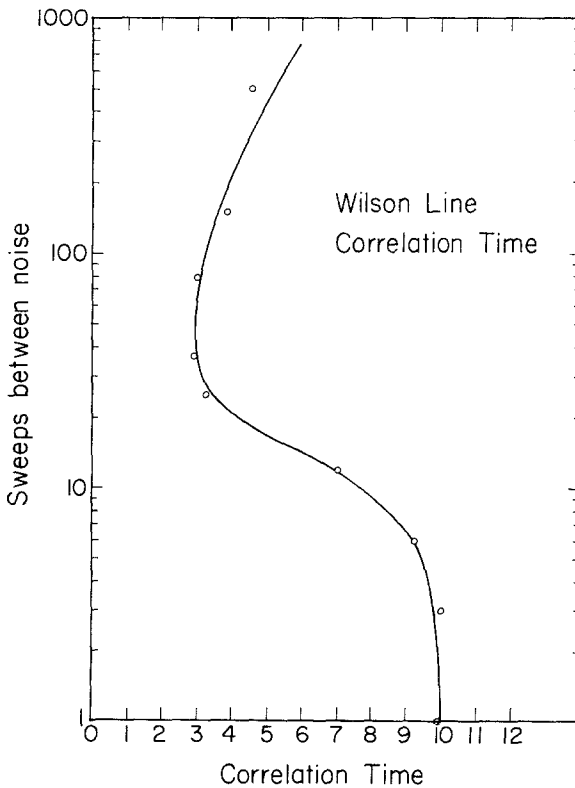


Fig. 1. Time correlation length vs sweeps between Langevin updates.

5. BEATING CRITICAL SLOWING DOWN

One of the most serious limitations of computer simulation studies of critical behavior is the need to run programs longer on larger lattices as the parameters of one's lattice system are tuned closer to the system's critical point. Larger lattices are needed because the system's correlation length diverges at the critical point. Longer runs are needed because the time correlation length—the correlations between configurations as a function of the time parameter in the Langevin or microcanonical schemes—also diverges at the critical point. For stochastic methods such as ordinary Monte Carlo and Langevin algorithms, the time correlation length grows as the square of the ordinary correlation length. Therefore, to achieve the same accuracy in different simulation measurements of a d -dimensional physical system, the total computer time must grow as the $(d + 2)$ -power of the correlation length. This phenomenon is called critical slowing down and has limited the use of simulation methods significantly in the past.

Within the context of microcanonical and stochastic differential equations, such as the Langevin equation, there is an interesting proposal to eliminate critical slowing down.⁽¹²⁾ Consider the microcanonical Lagrangian for the planar spin model in two dimensions

$$L = \frac{1}{2} \sum_i \dot{\theta}_i^2 - \beta \sum_{\langle ij \rangle} \cos(\theta_i - \theta_j) \quad (5.1)$$

The trajectory $\{\theta_i(t), i = 1, 2, \dots, \text{number of sites}\}$ is computed numerically from the discrete form of the Euler-Lagrange equation for $\theta_i(t)$. One wants to choose the discrete step size dt large so that the trajectory explores phase space rapidly and efficiently. A higher-order Runge-Kutta algorithm might be employed to achieve this while maintaining good accuracy. The rapidly varying ultraviolet modes in the system determine the largest possible time step permissible—if dt is too large the continuity in the time development of the ultraviolet modes is lost and the time evolution of the discrete system diverges. Accurate measurements of matrix elements which are sensitive to just the ultraviolet modes of the system are not the most interesting. Typically the physics of the critical point and the continuum limit of the lattice system is found at length scales on the order of the correlation length. These infrared modes are extremely smooth and their time evolution suffers from critical slowing down. One would like to evolve these spatially smooth modes with a large discrete time step while leaving the time step for the spatially erratic ultraviolet modes small. It is easy to introduce an effective time step whose size is momentum-dependent to accomplish this. Change the microcanonical Lagrangian to read

$$L = \sum_i \frac{1}{2} \dot{\theta}_i (\nabla^2 + m^2) \dot{\theta}_i - \beta \sum_{\langle ij \rangle} \cos(\theta_i - \theta_j) \quad (5.2)$$

Since we have only altered the kinetic piece of the Lagrangian and have left it quadratic in θ_i , the equilibrium microcanonical ensembles generated by (5.1) and (5.2) are identical. Considering (5.2) in momentum space we see that the effective time step behaves as

$$dt_{\text{eff}} = dt(p) = [dt_0/(p^2 + m^2)^{1/2}] \quad (5.3)$$

so the time step for the infrared modes, small p , will be suitably large if we choose m , an infrared cutoff, small. A similar improvement can be made in the Langevin equation for the planar model. Since the time step of the Langevin scheme is proportional to the square of the time step for the microcanonical scheme, the scaling relation reads

$$dt_{\text{eff}} = dt_0[(p^2 + m^2)_{\text{max}}/(p^2 + m^2)] \quad (5.4)$$

In practice the propagator $(p^2 + m^2)$ and its maximum value in (5.3) and (5.4) are replaced by their lattice counterparts.

Before considering the results of numerical experiments, consider two important technical issues here. First, the acceleration method presented here is based on free field theory, i.e., the replacement of $1 \rightarrow \nabla^2$ in (5.2) would be optimal for a free field theory. Therefore, it is possible that the method is not as effective as one would naively expect for interacting systems whose dynamics are highly nonlinear. In the case of the planar model, however, tests of the acceleration method, both above and below the Kosterlitz–Thouless transition where topologically significant vortices play an important role, have been very successful. The generality of naive acceleration methods will be interesting to understand. The second issue concerns the numerical implementation of the method. Since (5.2) involves ∇^2 in the kinetic energy, ∇^2 must be inverted at each time step to evolve the system $\{\theta_i(t)\}$ forward in time. This can be done by means of the fast Fourier transform (FFT) algorithm. The computer time for this operation grows as $cV \ln V$, where V is the number of degrees of freedom of the system and c is a constant of order unity. So, this additional ingredient in the algorithm slows it down negligibly. All supercomputers and array processors have highly tuned FFT routines in their libraries, so the scientific user can incorporate this new method into existing codes almost painlessly.

The results of a numerical study of the accelerated Langevin equation for the planar model are shown in Figs. 2 and 3. A 16×16 lattice was chosen and the temperature was set to 1.167, slightly above the Kosterlitz–Thouless critical point in the vortex phase. In Fig. 2a–c we show the time correlation function for high, medium, and low momentum components of the spin–spin correlation function. Note the critical slowing down here—the temporal correlation length for the low momentum mode of the

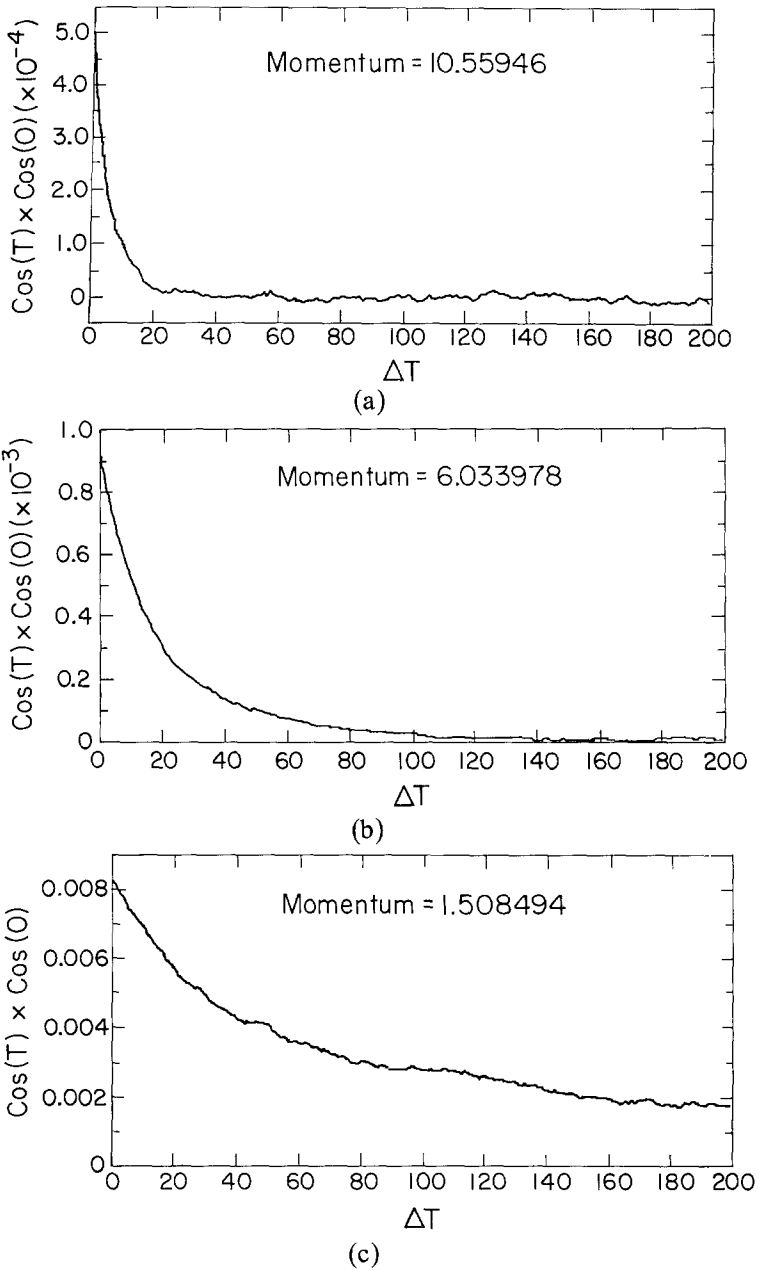
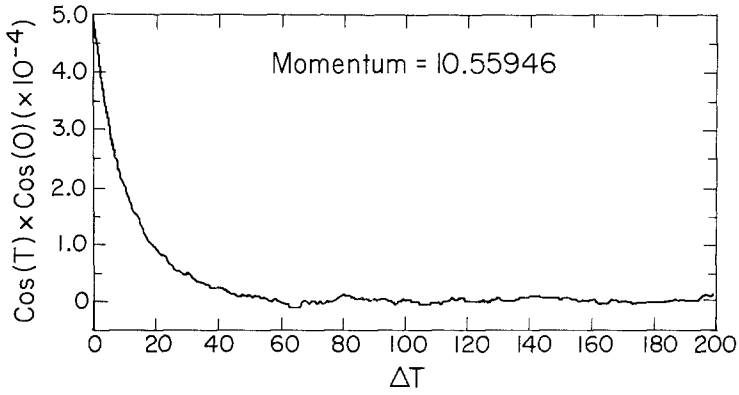
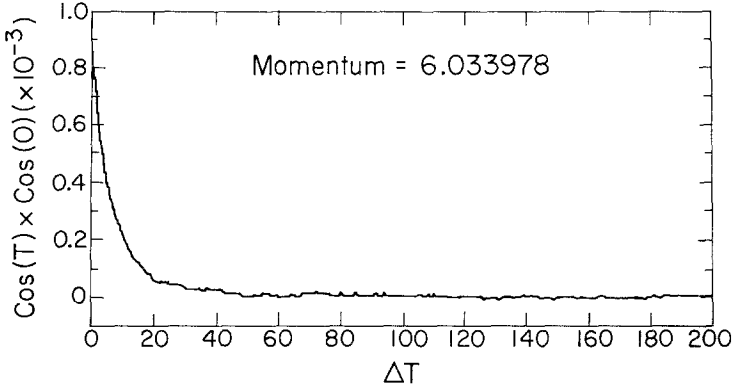


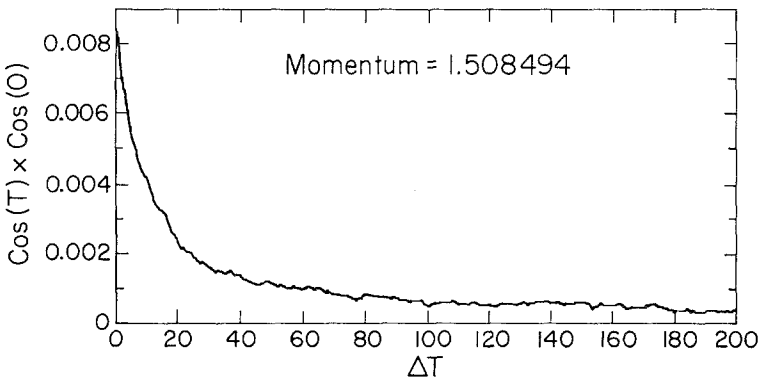
Fig. 2. The time correlation function of the high, medium, and low momentum components of the spin-spin correlation function of the planar model are shown. The naive Langevin algorithm was used.



(a)



(b)



(c)

Fig. 3. Same as Fig. 2, except the algorithm has been accelerated.

correlation function is almost an order of magnitude greater than that for the high momentum mode. In Fig. 3a-c we again show the time correlation function for the spin-spin correlation function, but now the algorithm has been accelerated. Note that the temporal correlation lengths are independent of momentum, as advertised!

The generalization of the acceleration procedure to gauge theories is particularly important because the spatial dependence of composite propagators must be measured well to determine the masses of the states of quantum chromodynamics. This problem is under study.

6. QUANTUM CHROMODYNAMICS SIMULATIONS

Now let's discuss the status of large scale simulations of $SU(2)$ and $SU(3)$ gauge theories with four light, dynamical Dirac fermions—simulations close to the real theory QCD. Various projects are in progress.

First is the thermodynamics of the continuum field theory. Here one wants to understand QCD at finite temperature and study the transition from hadronic matter to a quark-gluon plasma. One wants to know if there are true nonanalyticities in the thermodynamic quantities of interest

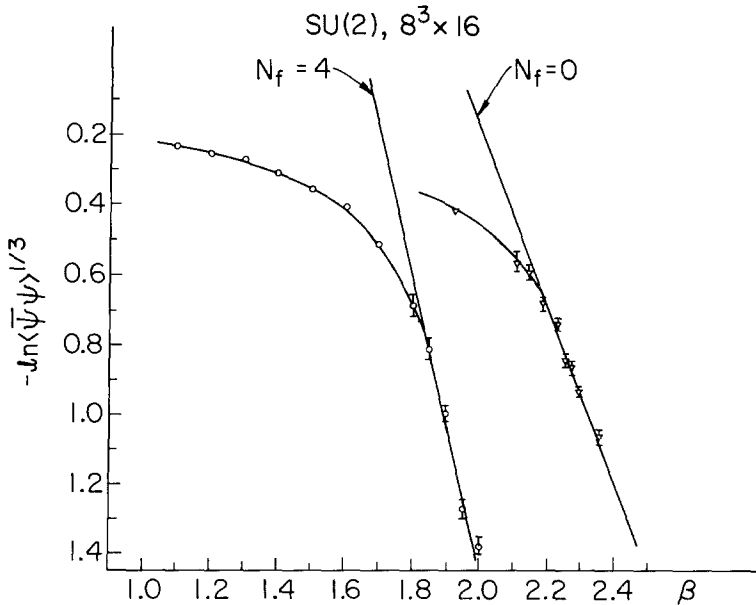


Fig. 4. Scaling curves of $\langle \bar{\psi}\psi \rangle$ vs β with $N_f=0$ (quenched) and $N_f=4$.

such as the entropy and internal energy densities. The $SU(2)$ and $SU(3)$ theories without fermion feedback showed such nonanalyticities, and their behavior is well-understood in the context of traditional statistical mechanics. The situation is relatively unclear when fermion feedback is accounted for and the subject is quite controversial. A chiral restoring transition is certainly present, but fermion screening may be qualitatively similar for all temperatures rendering the thermodynamics of the “transition” smooth. This is particularly interesting question for the groups developing fermion algorithms, because they are completely dependent on numerical methods for the answers to these physics questions.

The $SU(2)$ theory has been studied on a 6×12^3 lattice at six β values and three fermion mass values (0.10, 0.075, and 0.050) with $5 \cdot 10^3$ to 10^4 sweeps of the microcanonical algorithm for each point. The $SU(2)$ spectrum has been studied similarly on a $8^3 \times 16$ lattice, and an analogous $SU(3)$ project is underway.

In Fig. 4 we show the scaling regions of the pure $SU(2)$ theory and the theory with $N_f=4$ species of fermions. The agreement with asymptotic

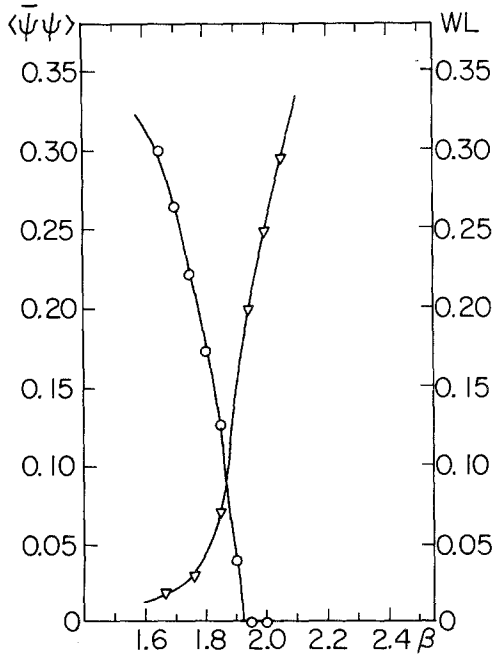


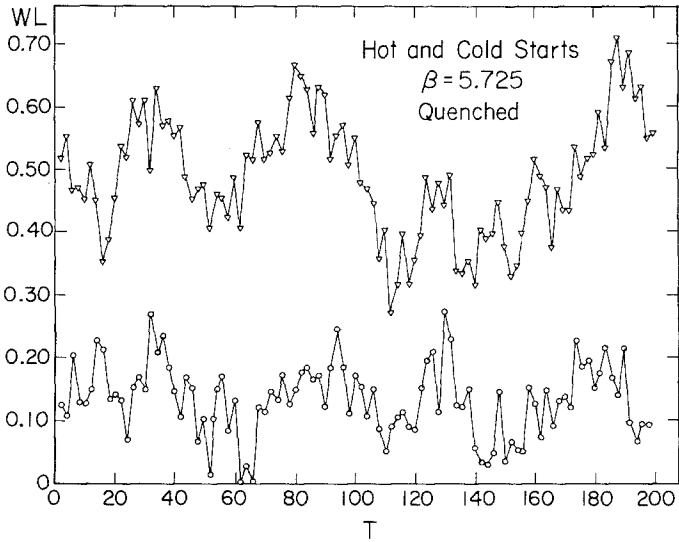
Fig. 5. $\langle \bar{\psi}\psi \rangle$ and WL (Wilson line) vs β on a 6×12^3 lattice for $SU(2)$ gauge theory with four species f quarks.

freedom for $\langle \bar{\psi}\psi \rangle$ is quite nice. Note that fermion feedback shifts the $\langle \bar{\psi}\psi \rangle$ curve toward stronger coupling as N_f is increased *and* the slope of $\ln\langle \bar{\psi}\psi \rangle$ vs β changes appropriately. It appears that the scaling region for the $N_f=4$ theory begins at $\beta=1.85$.

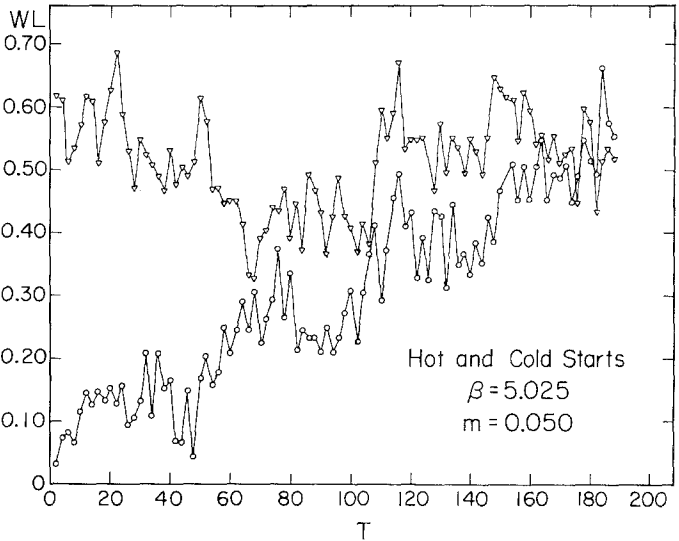
In Fig. 5 we show $\langle \bar{\psi}\psi \rangle$ extrapolated to zero mass and the Wilson line (WL) for a 6×12^3 lattice in the $SU(2)$, $N_f=4$ theory. It appears that the transition from hadron to quark-gluon matter is abrupt. It is crucial to confirm or refute this result with other algorithms.

Further evidence for this picture of the thermodynamics of quarks and gluons comes from applications of the hybrid algorithm.⁽¹³⁾ We consider $SU(3)$ gauge theory with four species of quarks.

The lattice theory was simulated on a 4×8^3 lattice with bare quark masses of 0.10, 0.075, and 0.050 so that zero mass extrapolations could be done. We expect a fluctuation-induced chiral symmetry-restoring transition in the continuum limit. However, although the pure $SU(3)$ gauge field has a first-order deconfining phase transition signaled by a discontinuous Wilson line, that behavior should not persist in the theory with dynamical quarks because quark pairs screen long-range color forces at all temperatures. However, the chiral symmetry-restoring transition could result in a discontinuous change in the dynamically generated quark mass which could effect the thermodynamics of the system dramatically. We located the critical couplings β for both the pure gauge theory and the full theory with light quarks. The pure gauge theory showed a clear first-order deconfining transition at $\beta = 5.725 \pm .025$ and the full theory with a bare quark mass $m=0.050$ had a chiral symmetry-restoring transition at $\beta = 5.000 \pm .025$. The characters of these transitions were compared by searching for metastable states, as shown in Fig. 6. In Fig. 6a we show the time history of the Wilson line for the pure gauge theory at $\beta = 5.725$ for both a confined and an unconfined initial configuration. Ten thousand sweeps of the algorithm were run with $dt = .02$ with noise applied every .75 time units to the \hat{U} fields. The two-state signal in Fig. 6a is clear evidence for a first-order transition. The same procedure was followed for the theory with light fermions at $\beta = 5.025$ and the evidence for a hard first-order transition is lost as shown in Fig. 6b. However, as shown in Fig. 7, the transition between the hadronic and quark-gluon phases is very abrupt—the energy density ε/T^4 , for example, changes from 0.00 ± 5.00 to 42 ± 4.0 as β changes from 5.000 to 5.025. If asymptotic freedom applies to this data, the fractional change of the physical temperature over this β interval is only 3.8%. The statistics accumulated and the resolution in β are far superior to earlier simulations, and they strengthen the controversial result that the finite temperature transition in quantum chromodynamics is abrupt.



(a)



(b)

Fig. 6. (a) Time history of the Wilson line at the first-order phase transition of the pure gluon theory. (b) A time history in the theory with fermion feedback.

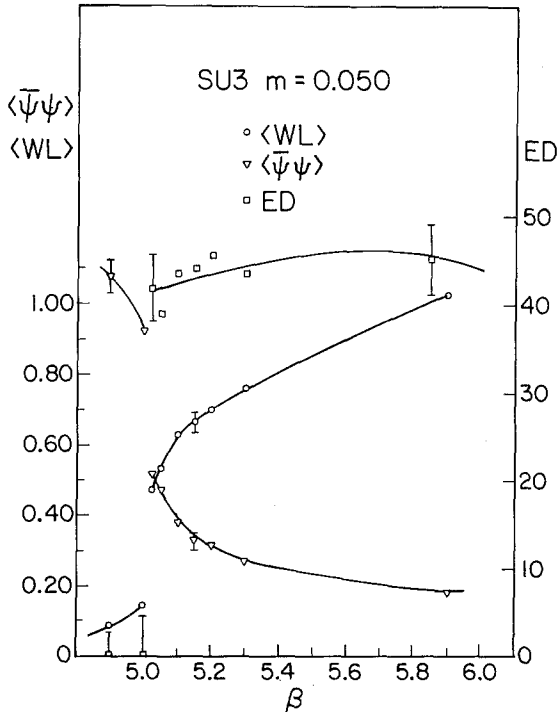


Fig. 7. $\langle \bar{\psi}\psi \rangle$, WL, and ED, the energy density measured in units of the fourth power of the temperature, on a 4×8^3 lattice for $SU(3)$ gauge fields with four species of quarks.

7. HIERARCHY PROBLEMS IN UNIFIED GAUGE THEORIES

We want to illustrate that lattice methods can be applied to theories "beyond QCD" which might have interesting mass scales at arbitrarily high energies. Unfortunately, the most interesting schemes involve chiral fermions and these cannot be attacked by lattice methods because we cannot place a single neutrino on the lattice with a conventional action. Anyway, in the realm of vector theories we can ask whether a theory can support disparate mass scales without the need to fine-tune a fundamental parameter. Chiral symmetry breaking and asymptotic freedom can conspire to do this, as suggested in the present context by Raby, Dimopolous, and Susskind.⁽¹⁴⁾ By considering single gluon exchange, they suggest that when $C_f g^2 \sim O(1)$ massless fermions of color charge, C_f will condense into a chiral condensate. By asymptotic freedom, this criterion leads to an exponential sensitivity of the characteristic energy scale of the condensate to the fermion's color charge. Changes of scale of $10^5 - 10^{10}$ are possible in such "technicolor" schemes, although realistic models do not exist.

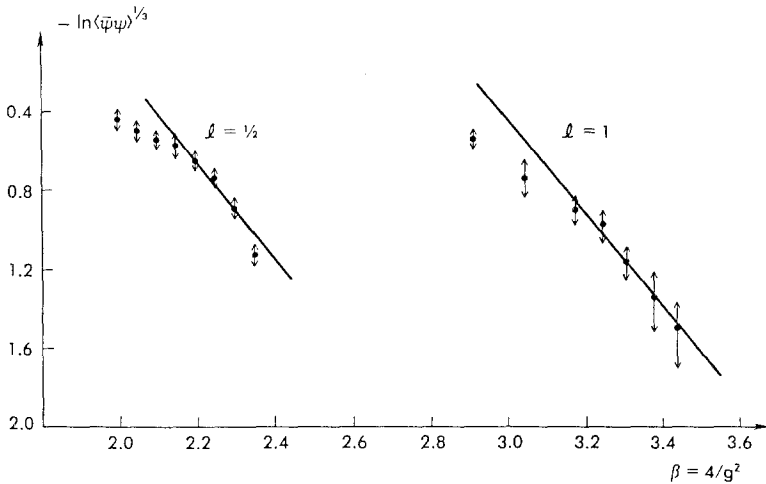


Fig. 8. $l = \frac{1}{2}$ and 1 condensates in the $SU(2)$ $N_f = 0$ theory.

The validity of the underlying feature of the scenario, that $C_f g^2 \sim O(1)$ leads to condensation, can be tested by lattice methods. In Fig. 8 we show data for the pure $SU(2)$ theory ($N_f = 0$) in which fundamental and adjoint condensates have been measured. The $l = 1$ condensation occurs at much weaker coupling (shorter physical distances) in general support of the scenario.

The next question is: Does this hierarchal structure survive the inclusion of fermion feedback? Let's consider the answer in two different models. First we can simulate $SU(2)$ with $N_f = 4$ Majorana quarks.⁽¹⁵⁾ Two mass scales can be searched for by simulating the theory at finite temperature and measuring $\langle\bar{\psi}\psi\rangle$ for the $l = 1$ quarks and the string tension for $l = \frac{1}{2}$ static quarks. In Fig. 9 we show data from a 4×8^3

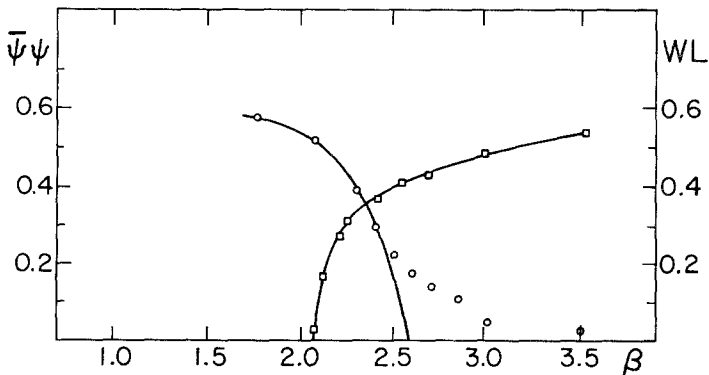


Fig. 9. $\langle\bar{\psi}\psi\rangle$ and the Wilson line for the $SU(2)$ theory with adjoint quarks.

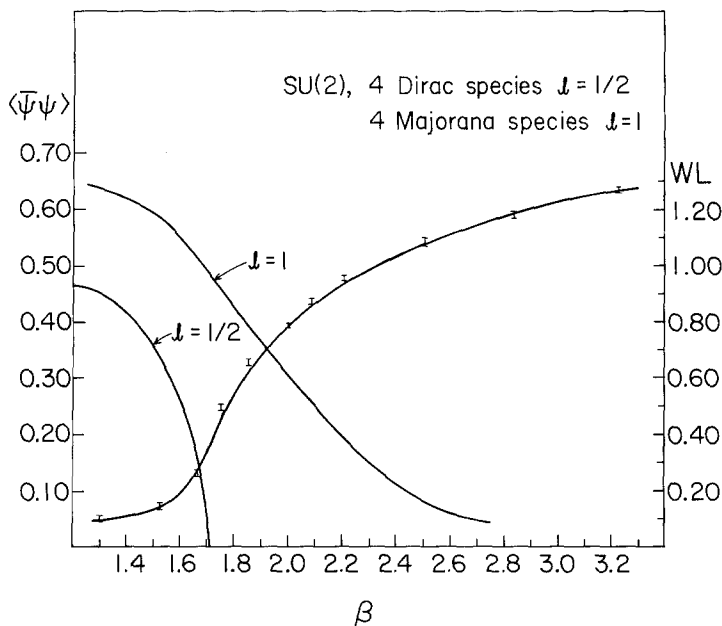


Fig. 10. $l = \frac{1}{2}$ and 1 condensates, and the Wilson line vs β in the $SU(2)$ theory with fermion feedback.

simulation depicting $\langle \bar{\psi}\psi \rangle$ and the Wilson line. Clearly the deconfinement and the chiral symmetry restoration temperatures are distinct. This is an encouraging result.

Finally, we can simulate a model with so much fermion feedback that asymptotic freedom is lost but the problem of multiple energy scales can be posed in the cutoff theory anyway. Consider $SU(2)$ with four flavors of fundamental Dirac fermions and four flavors of adjoint Majorana fermions. The results of a finite temperature simulation (4×8^3 lattice) are shown in Fig. 10 and support the hierarchy picture.

8. LATTICE GAUGE THEORY WITH MANY FLAVORS

Studies of the type described in the previous sections lead us to consider the phase diagram of lattice theories in the variables N_f and g^2 . It is then natural to ask about phase transitions in the $N_f - g^2$ plane and how they effect the $N_f = 2, 3$, and 4 simulations of most direct relevance of QCD. In Fig. 11 we show a speculative phase diagram.⁽¹⁷⁾ How does one

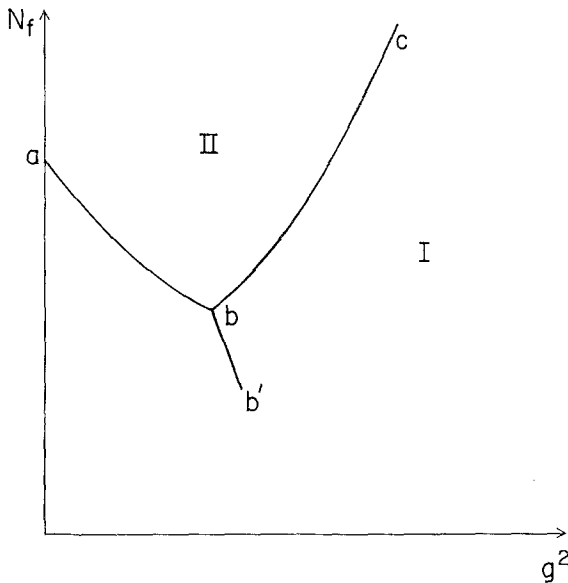


Fig. 11. Speculative phase diagram for $SU(3)$ lattice gauge theory with dynamical fermions. In region II, $\langle \bar{\psi}\psi \rangle = 0$; otherwise $\langle \bar{\psi}\psi \rangle \neq 0$.

arrive at such a guess? Along the N_f axis we can consider the continuum theory's Callan-Symanzik function

$$\beta(g) = -\beta_0 \cdot \frac{g^3}{16\pi^2} - \beta_1 \cdot \frac{g^5}{(16\pi^2)^2} \tag{8.1a}$$

where

$$\beta_0 = 11 - 2N_f/3 \quad \beta_1 = 102 - 38N_f/3 \tag{8.1b}$$

Note that β_0 changes sign at $N_f = 16.50$ and β_1 changes sign at $N_f = 8.05$. For $N_f > 16.50$ and $g^2 \approx 0$ the theory is not asymptotically free, so a small g^2 at short distances gives rise to a yet smaller g^2 at larger distances. This strongly suggests that $\langle \bar{\psi}\psi \rangle = 0$ in this region of the phase diagram. However, for large N_f and large g^2 , strong coupling expansions simply that $\langle \bar{\psi}\psi \rangle \neq 0$. These last two observations suggest that the $N_f - g^2$ phase diagram separates into two parts labeled with the order parameter $\langle \bar{\psi}\psi \rangle$.

Note that if the $\langle \bar{\psi}\psi \rangle = 0$ region dips, as shown in Fig. 11, the crossover from strong to weak coupling of the $N_f = 3$ theory will be effected by the nearby structure. It is natural to speculate that very abrupt crossover phenomena is present in the $N_f = 3$ theory as a consequence of

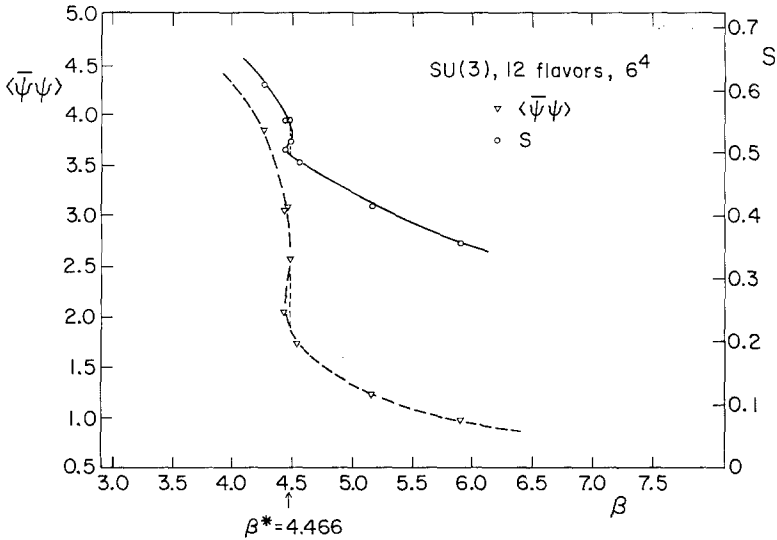


Fig. 12. $\langle \bar{\psi}\psi \rangle$ and the action for the $SU(3)$ theory with $N_f=12$ on a 6^4 lattice.

the rich $N_f - g^2$ phase diagram. Such effects may obscure the approach to continuum behavior of asymptotically free theories with fermions.

Some evidence for the line of transitions of Fig. 6 has already appeared in computer simulations.⁽¹⁷⁾ Figure 12 shows a microcanonical simulation of $SU(3)$ with $N_f=12$ on a 6^4 lattice. A clear signal for a first-order transition as a function of β is seen. In fact, this figure reminds us of a useful feature of microcanonical simulations: The absence of energy fluctuations can stabilize metastable states on finite systems leading to particularly clear evidence for first-order transitions⁽⁷⁾

Further studies of this type should elucidate Fig. 11. Simulations at variables N_f should reach the small g^2 , $N_f \sim 8-16$ region of the diagram where little theoretical insight is available. For large N_f and large g^2 the transition line is expected to be first-order,⁽¹⁶⁾ as found in Fig. 12.

9. FUTURE DIRECTIONS

The field of computer simulations of fermion systems is in its infancy. Algorithm development, testing, and error analysis, are crucial projects here. This is a controversial field at the moment and direct comparisons of different fermion algorithms are needed before proceeding to additional applications.

With a reliable algorithm in hand it will be particularly interesting to study the mass spectrum of QCD with fermion feedback. The validity of

the naive quark model and the role of the axial anomaly and topology in the spectrum and thermodynamics will become topics of study. The brute force measurement methods of present-day studies will be sorely tested by fermion feedback. For example, multi-pion states will appear in composite quark propagators and will interfere with the mass estimates of resonance states such as the meson. We will probably have to develop more subtle simulation methods which can extricate resonance states from the continuum to make a direct assault on the hadron spectrum, as done for the $SU(3) N_f=0$ theory.

Progress in the field over the next six months should clarify some of these questions.

ACKNOWLEDGMENT

This work is partially supported by the National Science Foundation under grant number NSF-PHY82-01948.

REFERENCES

1. K. G. Wilson, *Phys. Rev. D* **14**:2455 (1974).
2. J. B. Kogut and L. Susskind, *Phys. Rev. D* **9**:3501 (1974); *Phys. Rev.* **D11**:395 (1975).
L. Susskind, *Phys. Rev.* **D16**:3031 (1977).
3. D. Weingarten and S. Petcher, *Phys. Lett. B* **99**:33 (1981); F. Fucito, E. Marinari, G. Parisi, and G. Rebbi, *Nucl. Phys. B* **180**[FS2]:369 (1981).
4. D. Callaway and A. Rahman, *Phys. Rev. Lett.* **49**:613 (1982).
5. J. Polonyi and H. W. Wyld, *Phys. Rev. Lett.* **51**:2257 (1983); J. Polonyi, H. W. Wyld, J. B. Kogut, J. Shigemitsu, and D. K. Sinclair, *Phys. Rev. Lett.* **53**:644 (1984).
6. A. Guha and S.-C. Lee, *Phys. Rev. D* **27**:2412 (1983); A. Ukawa and M. Fukugita, *Phys. Rev. Lett.* **55**:1854 (1985).
7. J. Kogut, J. Polonyi, J. Shigemitsu, D. K. Sinclair, and H. W. Wyld, *Nucl. Phys. B* **251** [FS13]:311 (1985).
8. M. Creutz, *Phys. Rev. Lett.* **50**:411 (1983).
9. S. Nosé, *Molec. Phys.* **52**:255 (1984); J. Kogut and D. K. Sinclair, preprint (University of Illinois, Oct., 1985).
10. R. W. Hall and B. J. Berne, *J. Chem. Phys.* **81**:3641 (1984).
11. S. Duane, *Nucl. Phys. B* **257** [FS14]:652 (1985).
12. G. Batrouni et al., preprint (Cornell, CLNS-85(65), May 1985); G. Parisi, Les Houches Summer School, 1982.
13. S. Duane and J. B. Kogut, preprint (University of Illinois, October, 1985).
14. S. Raby, S. Dimopoulos, and L. Susskind, *Nucl. Phys. B* **169**:373 (1980).
15. J. Kogut, J. Polonyi, D. K. Sinclair, and H. W. Wyld, *Phys. Rev. Lett.* **54**:1980 (1985).
16. J. Banks and A. Zaks, *Nucl. Phys. B* **196**:189 (1982).
17. F. Fucito, S. Solomon, and H. Hamber, *Phys. Lett. B* **150**:285 (1985); J. Kogut, J. Polonyi, D. K. Sinclair, and H. W. Wyld, *Phys. Rev. Lett.* **54**:1475 (1985).